

## Prediction by artificial neural network of insulation performance of eco-treated cork stoppers: Experimental measurement, modeling and optimization

Tayeb Kermezli<sup>1\*</sup>, Mohamed Announ<sup>1</sup>, Aboubakr Boukrida<sup>1</sup>, Mustapha Douani<sup>2</sup>

<sup>1</sup>Materials and Environment Laboratory, Faculty Tech. Medea University, Algeria; kermezli.tayeb@univ-medea.dz (T.K.)  
announ.mohamed@univ-medea.dz (M.A.) boukridaaboubakr6@gmail.com (A.B.)

<sup>2</sup>LCVVE, Faculty Tech. Univ.HB, Chlef, Algeria; douani\_mustapha@yahoo.com (M.D.)

**Abstract:** This study aims to predict by artificial neural networks (ANN) the improvement in mass insulation of cork stoppers treated by high temperature thermal (HTT) and/or boiling. Experimental tests have shown that the desorption kinetics are more favorable for smaller molecules  $D_{KCl} < D_{NaCl}$ . The results validated the developed mathematical model, which accounted for the actual cylindrical shape of the stopper, and quantified the improvement in apparent diffusion coefficients as a function of the maximum temperature of the treatment cycle:  $D_{105^{\circ}} < D_{200^{\circ}} < D_{350^{\circ}} \approx D_{450^{\circ}}$  and the protocol type:  $D_A < D_B < D_C$ . The results revealed a positive correlation between temperature and the diffusion phenomenon, with a significant influence observed up to 350 °C. Furthermore, to enhance the accuracy of Dapp, the Bat Algorithm optimization method was applied, achieving a precision of the order of  $10^{-5}$ . An experimental database, composed of 3864 points, was previously optimized to be integrated into an artificial neural network (ANN) model with a specific architecture (5-5-6-1). The model thus developed demonstrated remarkable reliability, displaying a coefficient of correlation  $R^2$  of 0.9997 and an extremely low root mean square error (RMSE), evaluated at  $7.38 \times 10^{-14}$ . These performances underline the robustness and accuracy of the proposed model for the prediction of the studied phenomenon.

**Keywords:** ANN, Cork, Mass diffusion, Modeling, Optimization, THT.

### 1. Introduction

The study of fluid flow in heterogeneous and anisotropic porous media, such as cork stoppers, highlights the importance of material management and selection for insulation purposes [1-3]. Traditionally, this management has focused on the mechanical requirements of the materials [4]. This research concentrates on improving the insulation performance of cork stoppers through an eco-friendly high-temperature and boiling treatment, to make them competitive with other polymeric materials [3]. Cork is primarily extracted from the bark of the cork oak (*Quercus suber*), from Mediterranean tree species. This natural material has diverse applications in many industrial sectors, including the wine industry (bottle stoppers [5]), construction (thermal and acoustic insulation [6, 7]), fashion (accessories and footwear [8]), and the manufacture of decorative items and everyday objects. Its versatility and unique properties make it a sought-after renewable resource, meeting the demands of ecology, sustainability, and innovation in these fields.

Cork is characterized by marked anisotropy, making it a highly complex material. Furthermore, it exhibits a hygroscopic nature: its water content changes dynamically depending on humidity conditions, temperature, environment, and soil properties, thus influencing its physicochemical properties [9]. These variations in water content can also affect its mechanical performance and long-term behaviour, particularly in structural or insulation applications.

Optimizing the properties of certain porous biomaterials, as well as their preservation, relies primarily on chemical processes [10]. These methods also include high-temperature heat treatments, which are increasingly important in the fields of thermal and acoustic insulation, particularly with a view to energy efficiency and environmental sustainability. It should be noted that applying a high-temperature heat treatment to a porous biomaterial, such as cork, induces significant changes in its physical and chemical properties. These transformations give the material increased biological resistance to decay, while potentially improving its mechanical properties and dimensional stability. Furthermore, these heat treatments can also modify the microstructure of cork, reducing its porosity and increasing its bulk density, which may influence its performance as an insulating material. These modifications thus open up interesting prospects for the use of cork in innovative applications, while meeting growing demands for sustainability and environmental friendliness.

The enhancement is quantified by determining the apparent diffusion coefficient ( $D_{app}$ ) for different chemical species (NaCl or KCl) using conductometric methods [11] through various treatment cycles: 105°C, 200°C, 350°C, and 450°C, in contrast to other studies using pure water or gas [12]. Additionally, this study aims to extend the work of Seibert, et al. [13] and Brazinha, et al. [12] by comparing the natural and treated states of cork.

The goal is to develop a competitive biomaterial for insulation by improving its mechanical structure through various parameters, including treatment temperature, treatment protocol, and the nature of the solution (NaCl and KCl) [1] as there are other parameters, such as the cork plantation area, to consider [14, 15]. By employing conductometric techniques, experimental results in transient modes are calibrated using a developed mathematical model to determine the apparent diffusion coefficient ( $D_{app}$ ), according to the algorithm in figure 1. It should be noted that the effect of the treatment on cork is directly related to the value of  $D_{app}$ . Given the numerous parameters influencing the insulating properties of the material, the analysis is refined using an artificial neural network (ANN) model, which will enable the prediction of various material properties without requiring new practical experiments for each sample [16].

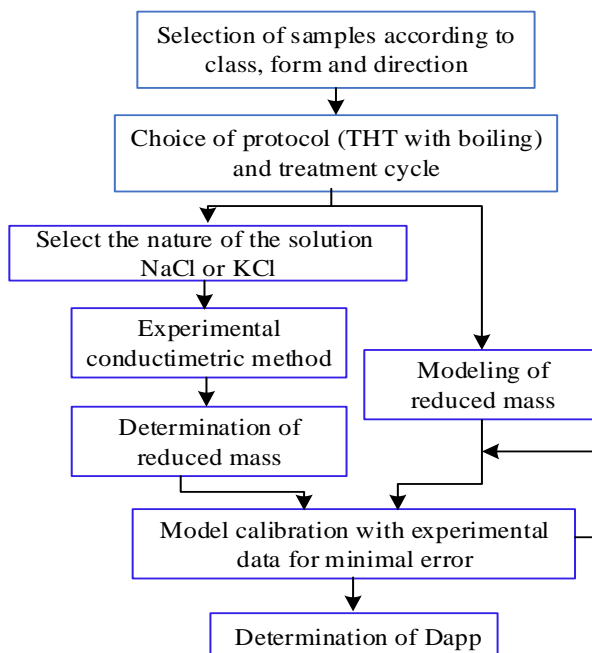


Figure 1.  
Organigramme de détermination du  $D_{app}$ .

## 2. Materials and Methods

Cork stopper samples were collected from the "EPE Jijel. Cork Waterproofing SPA", Skikda region in Algeria. They were cut from the same cork slab in the same direction (tangential) and to the same dimensions (Figure 2).

The samples were treated by boiling and/or high temperature treatment (HTT). The THT is under inert gas (argon). A programmable furnace of the NABERTHERM type "MORE THAN HEAT 30-3000°C" from the mechanical laboratory "Military Polytechnic School" in Bordj el-Bahri, Algiers, Algeria was used, according to the cycles described in Figure 3, following the protocols specified according to Table 1.

The structural modifications of cork were characterized by Fourier transform infrared spectroscopy (FTIR), carried out in the materials and environment laboratory of the University of Medea [17] as well as by scanning electron microscopy (SEM) using a Quanta 250 device from the FEI company, available in the Scientific and Technical Research Center in Physico-Chemical Analysis EXPERTISE, located in Bou-Ismaïl, Tipaza, Algeria [18, 19]. These techniques made it possible to obtain detailed information on the chemical composition and surface morphology of cork, thus facilitating the analysis of structural modifications induced by thermal treatments [20, 21].

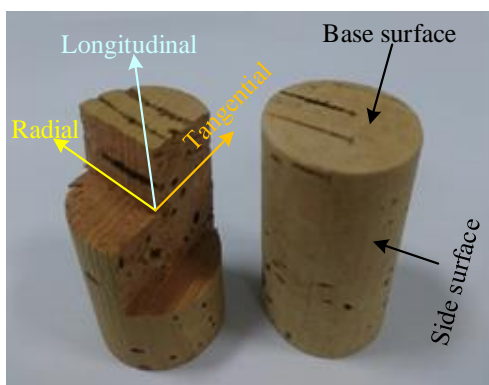


**Figure 2.**  
Photo of the caps used.

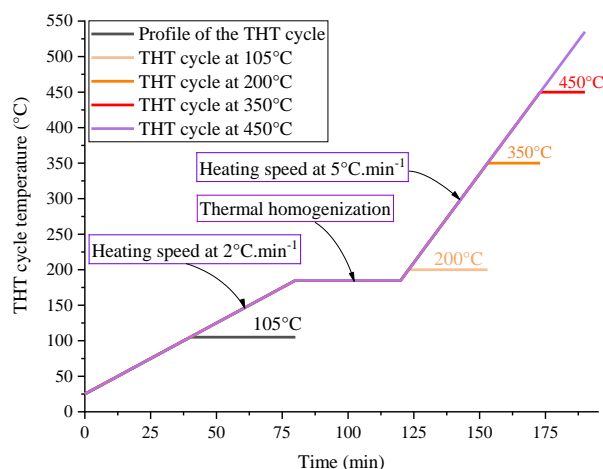


**Figure 3.**  
Different THT cycles at different heating rates.

**Table 1.**

Different variations of the experimental protocol.

Treatment	Protocol A	Protocol B	Protocol C
1st step	Boiling	THT	THT
2nd step	THT	Boiling	//

The conductimetric method was used to monitor the reduction in mass of the samples, while the desorption kinetics were tracked through conductimetric analysis of aqueous solutions. Factors such as treatment temperature, treatment protocol, and the nature of the diffusing species were considered for each test.

### 2.1. Modeling

To model the diffusion through the lateral surface of the cylindrical sample simplifying assumptions are adopted to facilitate the mathematical description of the phenomenon. This modelling is based on the establishment of a mass balance of the diffusing chemical species (i) through a differential volume element (dv) of the composite material. The mass balance is expressed after abstraction of any chemical reaction as well as the negligible contribution of convection, the mass balance equation is reduced to:

$$(\text{Accumulation term}) = (\text{Diffusion term}) \quad (1)$$

who gives

$$\frac{\partial c_i(r,t)}{\partial t} - D_{iapp} \left[ \frac{\partial^2 c_i(r,t)}{\partial r^2} - \frac{\beta}{r} \frac{\partial c_i(r,t)}{\partial r} \right] = 0 \quad (2)$$

The partial differential equation from the mass transfer balance is solved by adopting simplifying assumptions, as well as boundary and initial conditions adapted to the geometry of the cylinder sample characterized by a shape factor  $\beta=1$ . This approach allows the equation to be reduced to a system expressed in cylindrical coordinates. The final expression of the diffusion model, taking into account the real cylindrical shape of the sample, is given by:

$$\frac{m_t}{m_\infty} = \frac{4}{\sqrt{\pi}} \left( \frac{D_{iapp} \cdot t}{R^2} \right)^{1/2} - \frac{D_{iapp} \cdot t}{R^2} - \frac{1}{3\sqrt{\pi}} \left( \frac{D_{iapp} \cdot t}{R^2} \right)^{3/2} + \dots \quad (3)$$

Where:  $m_t$  is the mass of the substance released at time t,  $m_\infty$  is the mass of the substance transferred after complete desorption of the cork at infinite time, R is the radius of the stopper along the diffusion direction, and  $D_{iapp}$  is the apparent diffusion coefficient of the chemical species.

The mass diffusivity  $D_X$  ( $\text{cm}^2\text{s}^{-1}$ ) of the ion and cation X in water can be calculated using the Nernst-Einstein equation [22]:

$$\text{For potassium chloride (KCl)} : D_{K^+Cl^-/H_2O} = \frac{RT}{F^2} \frac{\frac{1}{\lambda_{Cl^-}^0} + \frac{1}{\lambda_{K^+}^0}}{\frac{1}{\lambda_{Cl^-}^0} + \frac{1}{\lambda_{K^+}^0}} = 6,689.10^{-8}T \quad (4)$$

$$\text{For sodium chloride (NaCl)} : D_{Na^+Cl^-/H_2O} = \frac{RT}{F^2} \frac{\frac{1}{\lambda_{Cl^-}^0} + \frac{1}{\lambda_{Na^+}^0}}{\frac{1}{\lambda_{Cl^-}^0} + \frac{1}{\lambda_{Na^+}^0}} = 5,403.10^{-8}T \quad (5)$$

Where:  $R = 8.3143$  [ $\text{J}(\text{mole.K})^{-1}$ ] is the ideal gas constant,  $F = 96488$  Coulomb is the Faraday constant,  $\lambda^0$  is the limiting equivalent conductivity of the anion and/or cation in water at  $25^\circ\text{C}$ , T is the temperature of the water (in Kelvin), and  $Z_X$  is the absolute value of the algebraic charge of the anion and/or cation.

This observation confirms the findings of Langford, et al. [23] which highlight the significant influence of molecular size on diffusion rates. More specifically, it highlights that the solute KCl, with a smaller molecular size, has a higher diffusion rate than NaCl. This difference can be explained by the smaller ionic radius of potassium ( $K^+$ ) compared to that of sodium ( $Na^+$ ), thus favoring an increased

mobility of KCl in the diffusion medium [24]. These conclusions are in perfect agreement with the theoretical predictions described by equations 2 and 3, which confirm the inverse relationship between the size of the ions and their diffusion rate.

## 2.2. Implementation of Artificial Neural Networks (ANN)

In this study, we developed a methodology to estimate the diffusion rate in cork under the operational conditions detailed in the experimental section, employing a statistical approach based on artificial neural networks (ANN). This predictive technique was chosen for its balance between simplicity and efficiency, as highlighted by Zhang, et al. [25]. To achieve this goal, we constructed an extensive experimental database comprising 3864 data points that encapsulate the primary operating parameters. However, this size must meet the requirements of the theoretical relationships given by Shalev-Shwartz and Ben-David [26] and Aggarwal [27].

The minimum database size required to train an artificial neural network (ANN) is estimated based on the number of model parameters. The total number of parameters  $N_{param}$  is given by:

$$N_{param} = \sum_{i=1}^{L-1} (n_i \times n_{i+1}) + \sum_{i=2}^L n_i \quad (6)$$

Where  $n_i$  represents the number of neurons in layer  $i$ . A rule of thumb suggests that the database size  $N_{data}$  should satisfy:

$$N_{data} \geq k \times N_{param} \quad (7)$$

With  $k$  generally between 5 and 10. This approach minimizes the risk of overfitting while ensuring effective model generalization.

These parameters include the time, the nature of the diffusing species, the treatment protocol, and the maximum temperature of the thermal treatment (THT) cycle. This database will serve as a basis for the design of an optimal ANN architecture by determining the most appropriate number of hidden layers and neurons to accurately predict the apparent diffusion coefficient  $D_{app}$ .

## 3. Results and Discussion

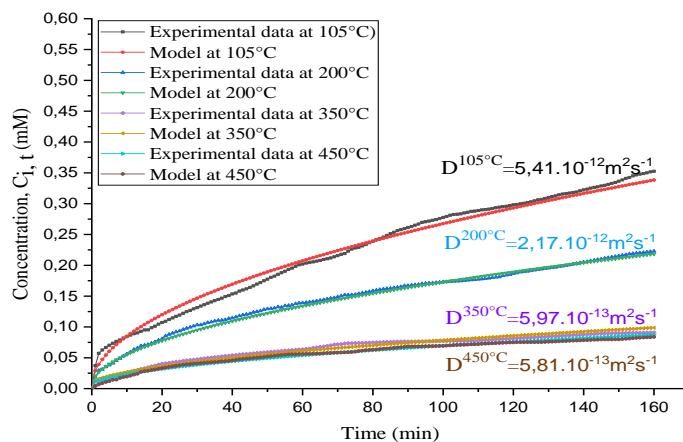
Figures 4 and 5 illustrate that the proposed model effectively captures the experimental behavior of the reduced mass under the influence of various parameters, including the maximum temperature of the thermal treatment cycle, the treatment protocol and the nature of the aqueous solution.

Figure 4 reveals a significant dependence of the apparent diffusion coefficient ( $D_{app}$ ) on the maximum temperature of the thermal heat treatment (THT), particularly up to 350 °C. Beyond this threshold, however, the temperature no longer exerts a measurable influence on the diffusion kinetics of the chemical species (NaCl), as evidenced by the convergence of  $D_{app}$  values:  $D_{105^\circ} < D_{200^\circ} < D_{350^\circ} \approx D_{450^\circ}$ .

This temperature-dependent behavior is further corroborated by the infrared (IR) spectroscopy analysis presented in Figure 6, which highlights the structural modifications induced by the thermal treatment. Specifically, the observed shifts in peak intensities in the IR spectra provide direct evidence of changes in the chemical structure of the material, consistent with the alterations in diffusion properties.

Additionally, the nature of the diffusing species (NaCl and KCl) plays a pivotal role in determining the mass transfer rate, with the degree of influence directly correlated to molecular size of the chemical species. This relationship is illustrated in Figure 5, where the  $D_{KCl}$  for KCl consistently exceeds that  $D_{NaCl}$  of NaCl, reflecting the differential mobility of the two species.

Furthermore, the timing of the THT protocol—whether applied before or after boiling, or as a standalone treatment significantly affects the mass isolation efficiency. As shown in the corresponding figure, the protocol involving THT prior to boiling (Protocol B) yields the highest  $D_{app}$  value, with the following hierarchy:  $D_B > D_C > D_A$ . These findings underscore the critical importance of optimizing treatment protocols to achieve enhanced mass transfer performance.



**Figure 4.**

Validation of the diffusivity model with experimentation under the effect of THT temperature.

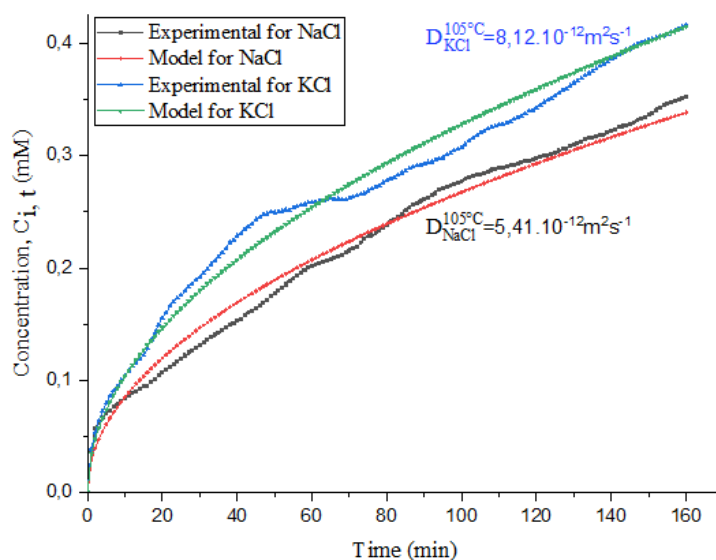


**Figure 5.**

Validation of the diffusivity model with experimentation under the effect of the nature of the solute.

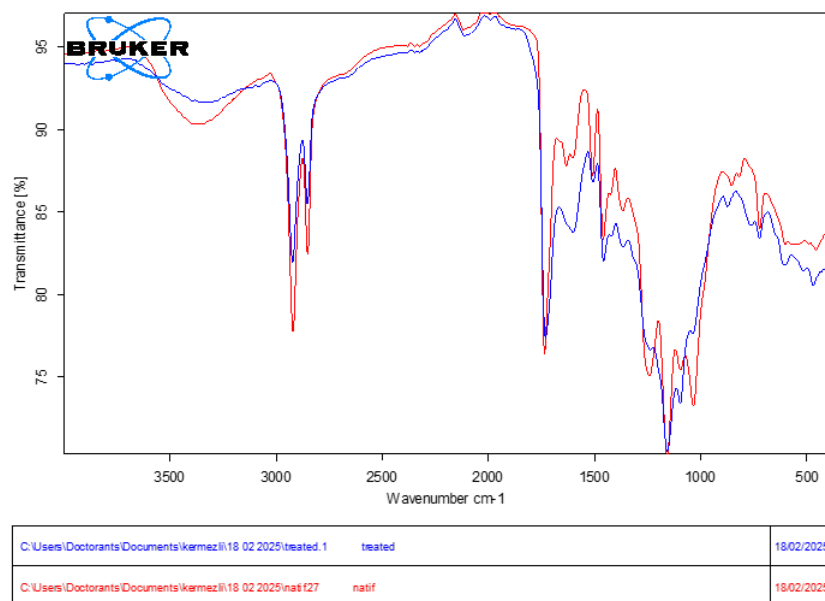


**Figure 6.**  
IR spectra of treated and native cork stopper.

Following model calibration using experimental data on reduced mass obtained by the conductometric method, the resulting apparent diffusion coefficients ( $D_{app}$ ) were optimized using the Bat algorithm [28]. This optimization process achieved a high level of accuracy, with a margin of error of the order of  $10^{-5}$ , as detailed in Table 2. The Bat algorithm, inspired by the echolocation behavior of bats, was chosen for its efficiency in solving complex optimization problems and its ability to converge quickly to optimal solutions. The strong agreement between model predictions and experimental data underlines the robustness of the proposed approach to accurately describe the diffusion phenomena studied. Furthermore, the minimal margin of error highlights the reliability of the calibration process and the suitability of the Bat algorithm for refining the model parameters. These results not only validate the theoretical framework but also provide a solid basis for further investigations into the influence of other variables on mass transfer processes. The optimized  $D_{app}$  values, presented in Table 2, provide an essential reference for further analyses and applications in related fields.

**Table 2.**

Diffusion coefficients in a cork stopper under the effect of the protocol, the temperature of the THT and the nature of the solute.

Protocol		A	B	C
Protocol with NaCl	$D_{NaCl}^{105^\circ}$	$5,41.10^{-12}$	$6,05.10^{-12}$	$5,80.10^{-12}$
	$D_{NaCl}^{200^\circ}$	$2,17.10^{-12}$	$2,63.10^{-12}$	$2,91.10^{-12}$
	$D_{NaCl}^{350^\circ}$	$5,9.10^{-13}$	$8,33.10^{-12}$	$7,14.10^{-12}$
	$D_{NaCl}^{450^\circ}$	$5,81.10^{-13}$	$7,42.10^{-12}$	$6,23.10^{-12}$
Protocol with KCl	$D_{KCl}^{105^\circ}$	$8,12.10^{-12}$	$8,97.10^{-12}$	$8,61.10^{-12}$
	$D_{KCl}^{200^\circ}$	$2,9.10^{-12}$	$3,71.10^{-12}$	$3,41.10^{-12}$
	$D_{KCl}^{350^\circ}$	$7,08.10^{-13}$	$9,32.10^{-12}$	$9,90.10^{-12}$
	$D_{KCl}^{450^\circ}$	$7,12.10^{-13}$	$9,04.10^{-12}$	$7,39.10^{-12}$

The learning model developed in this study is based on a multi-layer perceptron (MLP) architecture, designed to accurately predict  $D_{app}$  based on the various experimental parameters in Table

2. To identify the optimal neural network architecture, a series of systematic tests was performed, as detailed in Table 3. These tests consisted of evaluating different network configurations, varying the number of hidden layers (from one to three) and the number of neurons per layer (from 5 to 15). This methodical approach allowed us to explore a wide range of combinations to determine the structure offering the best predictive performance while avoiding overfitting.

Table 3 summarizes the key parameters involved in identifying the optimized model, obtained using ANN. This configuration made it possible to capture the nonlinear relationships between experimental parameters and  $D_{app}$  values, while minimizing prediction errors.

**Table 3.**

Proposed ANN model structure.

Network type	Algorithm	Input layer	Hidden layer de (1 à 3)		Output layer	
Feed-Forward Backpropagation	Levenberg-Marquardt ( <i>trainlm</i> )	Neurons number	Neurons Number for each	Activation function for each	Neurons number	Activation function
Neural Network						
(FFFBP NN, <i>newff</i> )		5	For 5 to 15	ReLU (poslin)	1	purelin

The graphs presented in Figure 7 illustrate that the implementation of the artificial neural network (ANN) is both satisfactory and robust.

This performance is attributable to the use of a substantial database, comprising 3864 points, which represents 529.3% of the recommended minimum size of 730 points calculated from equations 3 and 6 for the specific architecture (5-5-6-1), illustrated in Figure 8.

This conclusion is supported by correlation coefficients close to 1 (0.9998) for the different data analysis phases (training, validation, and testing), as well as by an extremely low root mean square error (RMSE) of around  $7.38 \times 10^{-14}$ .



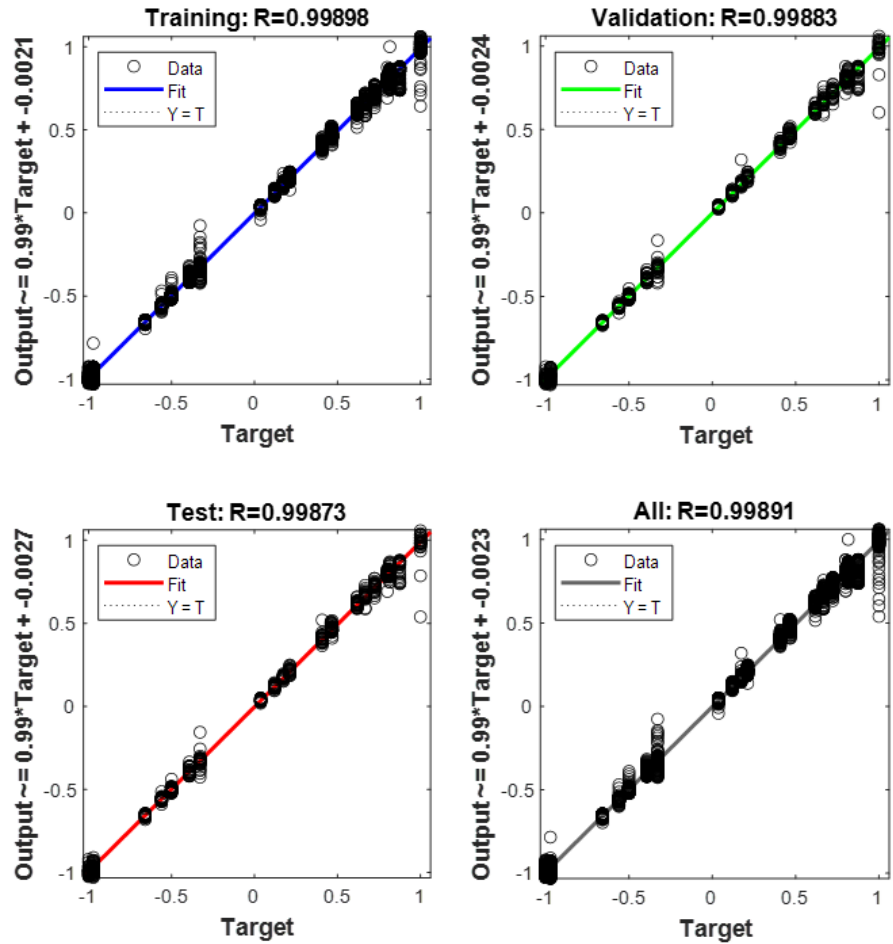


**Figure 7.**  
Regression performance output vs. Target with linear fit for different data subsets.

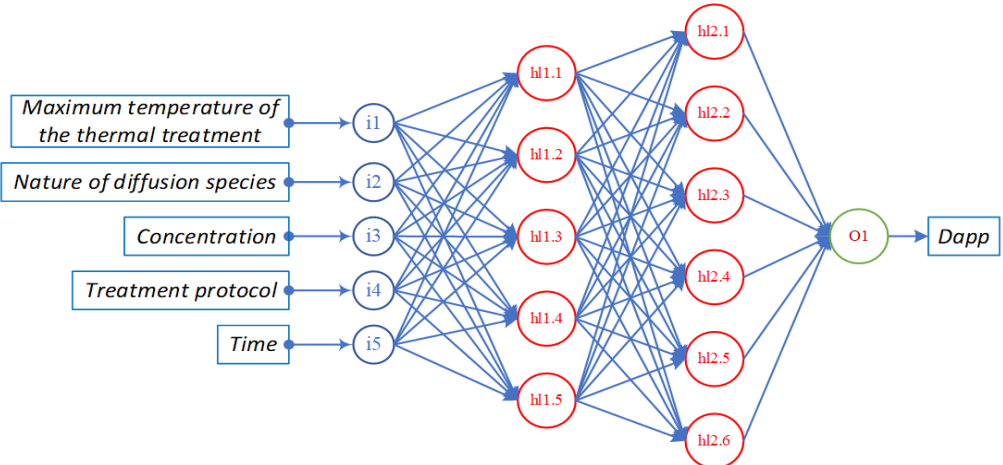


**Figure 8.**  
Architecture of the neural network.

These results demonstrate that the model is capable of capturing the complex relationships between input and output variables with high accuracy, while generalizing effectively to new data. Furthermore, the model performance, characterized by such a low RMSE, highlights the effectiveness of the optimization of the RNA architecture and the relevance of the selected parameters. These elements confirm the reliability of the proposed model and its potential for practical applications requiring high predictive accuracy.

Figure 9 illustrates that the gradient decreases globally over the course of iterations (epochs), indicating that the optimization process is converging toward a minimum of the cost function. The variations in  $\mu$  reflect the dynamic adaptation of the algorithm. When  $\mu$  decreases, the algorithm places greater trust in the local gradient trends, suggesting improved convergence. Furthermore, the absence of fluctuations in the validation phase demonstrates the network's strong generalization capability, even with a relatively low number of epochs (15).

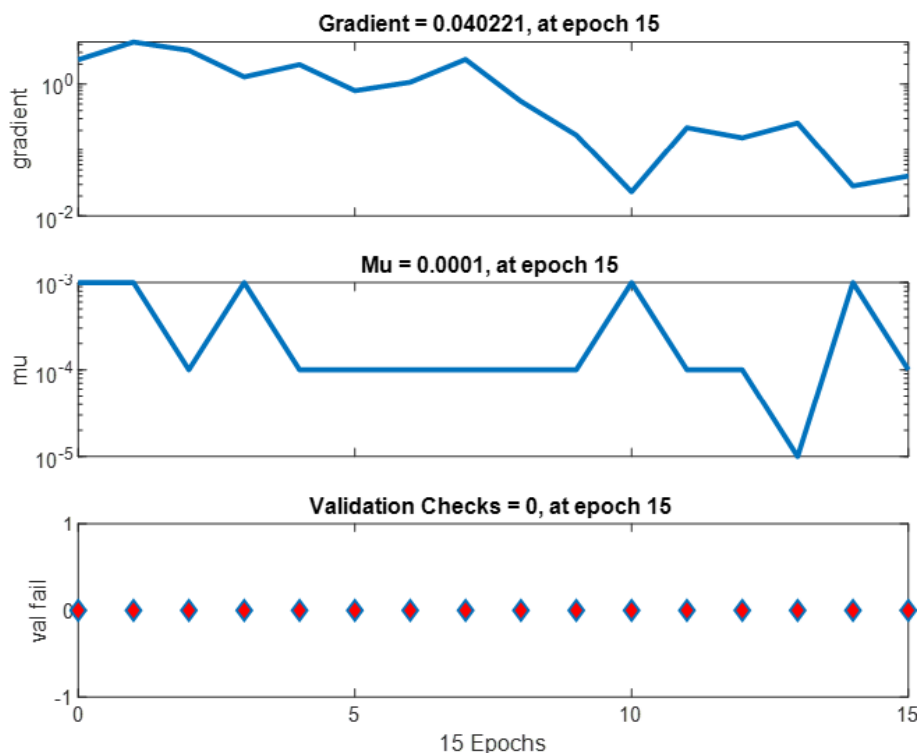


**Figure 9.**  
Evolution of Gradients, Learning Rate ( $\mu$ ), and Validation Values per Epoch.

#### 4. Conclusion

This study highlighted the significant impact of high-temperature thermal treatments (THT) and boiling processes on the mass insulation properties of cork stoppers. We successfully modeled the desorption kinetics, with experimental results validating the developed model, showing improved diffusion coefficients with increasing treatment temperatures, particularly beyond 350°C:  $D_{105^\circ} < D_{200^\circ} < D_{350^\circ} \approx D_{450^\circ} = 5,81 \cdot 10^{-13} \text{m}^2 \text{s}^{-1}$ . The findings confirmed that molecular size affects diffusion, with  $D_{\text{KCl}} > D_{\text{NaCl}}$ . Additionally, the study emphasized the crucial role of the treatment protocol on insulation performance, demonstrating that the sequence of THT and boiling directly influences mass insulation:  $D_A < D_C < D_B$ . The Dapp values were optimized using the Bat Algorithm, achieving a precision

of  $10^{-5}$ . Through these improvements, including an innovative treatment protocol and optimized cycle temperature, the final product (cork stopper) becomes highly competitive in the market.

The database used for neural network modeling allowed the definition of an optimal architecture (5-5-6-1), achieving exceptional accuracy, with a coefficient of determination  $R^2$  of 0.9997 and an extremely low root mean square error (RMSE) of  $7.38 \times 10^{-14}$ . This remarkable performance is partly explained by the substantial size of the experimental database, comprising 3864 data points, or 529.3% of the recommended size limit for this specific architecture. The results obtained confirm the reliability and effectiveness of the developed model, which positions itself as a powerful predictive tool for analyzing diffusion properties as a function of various parameters.

This study not only contributes to a better understanding of cork stopper processing processes, but also establishes a solid methodological framework for future work aimed at optimizing material quality and production methods in the cork industry. The successful application of a neural network in this context highlights its potential for predicting complex material behaviors, opening up innovative perspectives in materials science and quality control. These advances underscore the importance of artificial intelligence-based approaches to addressing current industrial and scientific challenges.

### Transparency:

The authors confirm that the manuscript is an honest, accurate, and transparent account of the study; that no vital features of the study have been omitted; and that any discrepancies from the study as planned have been explained. This study followed all ethical practices during writing.

### Copyright:

© 2025 by the authors. This open-access article is distributed under the terms and conditions of the Creative Commons Attribution (CC BY) license (<https://creativecommons.org/licenses/by/4.0/>).

### References

- [1] C. Leite and H. Pereira, "Cork-containing barks—A review," *Frontiers in Materials*, vol. 3, p. 63, 2017. <https://doi.org/10.3389/fmats.2016.00063>
- [2] J. A. Paulo and D. I. Santos, "Virgin cork colour and porosity as predictors for secondary cork industrial quality," *Industrial Crops and Products*, vol. 205, p. 117513, 2023. <https://doi.org/10.1016/j.indcrop.2023.117513>
- [3] M. E. Rosa and M. A. Fortes, "The cellular structure of cork," *Journal of Materials Science*, vol. 23, no. 3, pp. 879–885, 1988. <https://doi.org/10.1007/BF01153981>
- [4] H. Pereira, *Cork: Biology, production, and uses*. Netherlands: Elsevier, 2007.
- [5] M. S. Pino, I. M. Alconchel, and P. V. Castro, "Manufacture of sustainable cork stoppers for spirits through compression molding," presented at the International Joint Conference on Mechanics, Design Engineering & Advanced Manufacturing, Cham: Springer Nature Switzerland, 2024.
- [6] Ö. Yay, M. Hasanzadeh, S. F. Diltemiz, and S. Gürgen, *Cork agglomerates in acoustic insulation. In Cork-Based Materials in Engineering: Design and Applications for Green and Sustainable Systems*. Cham: Springer Nature Switzerland, 2024.
- [7] Ö. Yay, M. Hasanzadeh, S. F. Diltemiz, M. C. Kuşhan, and S. Gürgen, *Thermal insulation with cork-based materials. In Cork-Based Materials in Engineering: Design and Applications for Green and Sustainable Systems*. Cham: Springer Nature Switzerland, 2024.
- [8] P. Burgos Pintos, P. Marzo Gago, N. Fernández Delgado, M. Herrera, A. Sanz de León, and S. I. Molina, "Sustainable product design by large format additive manufacturing of cork composites," *Virtual and Physical Prototyping*, vol. 19, no. 1, p. e2386106, 2024. <https://doi.org/10.1080/17452759.2024.2386106>
- [9] M. J. Kwak, S. H. Lee, and S. Y. Woo, "Growth and anatomical characteristics of different water and light intensities on cork oak (*Quercus suber* L.) seedlings," *African Journal of Biotechnology*, vol. 10, no. 53, p. 10964, 2011. <https://doi.org/10.5897/AJB11.2846>
- [10] L. Lübert, T. Andreas, and P. Meier, "The fixation of new alternative wood protection systems by means of oil treatment," *Materials Science*, vol. 17, no. 4, pp. 402–406, 2011. <https://doi.org/10.5755/j01.ms.17.4.777>

- [11] A. Zemirline, T. Kermezli, M. Announ, and M. Douani, "Investigation of the effect of cutting directions on the improvement of mechanical parameters of treated cork by tht: experimental measurement, modelling and optimization of mass transfer.," *Mechanics*, vol. 28, no. 3, pp. 204–210, 2022. <https://doi.org/10.5755/j02.mech.26956>
- [12] C. Brazinha, A. P. Fonseca, H. Pereira, O. M. Teodoro, and J. G. Crespo, "Gas transport through cork: Modelling gas permeation based on the morphology of a natural polymer material," *Journal of Membrane Science*, vol. 428, pp. 52–62, 2013. <https://doi.org/10.1016/j.memsci.2012.10.019>
- [13] D. Seibert, H. P. Felgueiras, A. Módenes, F. Borba, R. Bergamasco, and N. C. Homem, "Application of cork as adsorbent for water and wastewater treatment using ciprofloxacin as pharmaceutical model," *International Journal of Environmental Science and Technology*, pp. 1–18, 2024. <https://doi.org/10.1007/s13762-024-05836-w>
- [14] F. Benmeriem, M. Douani, C. Fares, T. Kermezli, and M. Announ, "Contribution to the analysis of the influence of climatic and geographic factors on the average mechanical parameters of cork growing in North Africa: The Case of Algeria," *Letters in High Energy Physics*, pp. 6516–6525, 2024. <https://doi.org/10.31526/lhep.2024.651>
- [15] J. J. Camarero, Á. Sánchez-Miranda, M. Colangelo, and L. Matías, "Climatic drivers of cork growth depend on site aridity," *Science of the Total Environment*, vol. 912, p. 169574, 2024. <https://doi.org/10.1016/j.scitotenv.2023.169574>
- [16] H. Pereira, "The rationale behind cork properties: A review of structure and chemistry," *BioResources*, vol. 10, no. 3, pp. 437–447, 2018. <https://doi.org/10.15376/biores.10.3.437-447>
- [17] F. Kačík *et al.*, "Impact of thermal treatment and accelerated aging on the chemical composition, morphology, and properties of spruce wood," *Forests*, vol. 16, no. 1, p. 180, 2025. <https://doi.org/10.3390/f16010180>
- [18] H. Pereira and M. E. Rosa, "Scanning electron microscopy in cork structure evaluation," *Journal of Cellulosic Materials*, vol. 7, no. 1, pp. 34–42, 2009.
- [19] D. Pérez-Terrazas, J. R. González-Adrados, and M. Sánchez-González, "Qualitative and quantitative assessment of cork anomalies using near infrared spectroscopy (NIRS)," *Food Packaging and Shelf Life*, vol. 24, p. 100490, 2020. <https://doi.org/10.1016/j.fpsl.2020.100490>
- [20] M. A. Fortes, L. F. Nunes, and P. Oliveira, "Thermal degradation and structural analysis of cork," *Journal of Applied Polymer Science*, vol. 92, no. 2, pp. 945–951, 2004. <https://doi.org/10.1002/app.20045>
- [21] T. Kermezli, A. Bensmaili, K. Amokrane, and A. Gacemi, "Mechanical behavior of cork modified by heat treatment at high temperature," *Mechanics*, vol. 19, no. 4, pp. 424–428, 2013. <https://doi.org/10.5755/j01.mech.19.4.5053>
- [22] X. Lu, "Application of the Nernst-Einstein equation to concrete," *Cement and Concrete Research*, vol. 27, no. 2, pp. 293–302, 1997. [https://doi.org/10.1016/S0008-8846\(97\)00005-6](https://doi.org/10.1016/S0008-8846(97)00005-6)
- [23] J. F. Langford, M. R. Schure, Y. Yao, S. F. Maloney, and A. M. Lenhoff, "Effects of pore structure and molecular size on diffusion in chromatographic adsorbents," *Journal of Chromatography A*, vol. 1126, no. 1–2, pp. 95–106, 2006. <https://doi.org/10.1016/j.chroma.2006.05.042>
- [24] M. Liu, H. Guo, J. Luo, X. Gui, Y. Xing, and Y. Cao, "Investigation on the effect of metal cation radius on montmorillonite hydration: Combining experiments with molecular dynamics simulation," *Separation and Purification Technology*, vol. 353, p. 128474, 2025. <https://doi.org/10.1016/j.seppur.2024.128474>
- [25] G. Zhang, B. E. Patuwo, and M. Y. Hu, "Forecasting with artificial neural networks: The state of the art," *International Journal of Forecasting*, vol. 14, no. 1, pp. 35–62, 1998. [https://doi.org/10.1016/S0169-2070\(97\)00044-7](https://doi.org/10.1016/S0169-2070(97)00044-7)
- [26] S. Shalev-Shwartz and S. Ben-David, *Understanding machine learning: From theory to algorithms*. Cambridge University Press: United Kingdom, 2014.
- [27] C. C. Aggarwal, *Neural networks and deep learning*. Cham: Springer, 2018.
- [28] X.-S. Yang and X. He, "Bat algorithm: literature review and applications," *International Journal of Bio-Inspired Computation*, vol. 5, no. 3, pp. 141–149, 2013. <https://doi.org/10.1504/IJBIC.2013.055093>